1992

Relationship of AVHRR-NDVI to seasonal drought for an evergreen tropical rainforest in Ujung Kulon, Indonesia

Agus Hidayat
The University of Montana

RELATIONSHIP OF AVHRR-NDVI TO SEASONAL DROUGHT
FOR AN EVERGREEN TROPICAL RAINFOREST
IN UJUNG KULON, INDONESIA

By

AGUS HIDAYAT

B.S. Bogor Agriculture University (Indonesia), 1984

Presented in partial fulfillment of the requirements for
the degree of Master of Science in Forestry

UNIVERSITY OF MONTANA
1992

Approved by :

Chairman, Board of Examiners

Dean, Graduate School

--------- July 27, 1992
Date :

Hidayat, Agus, MS, Summer 1992 Forestry

RELATIONSHIP OF AVHRR-NDVI TO SEASONAL DROUGHT FOR EVERGREEN TROPICAL RAINFOREST IN UJUNG KULON, INDONESIA (62 pp.)

Director : Dr. E. Raymond Hunt, Jr.

In 1982-1983, drought led to serious fires in the evergreen tropical rainforests of Indonesia. The Advanced Very High Resolution Radiometer (AVHRR) on board the NOAA polar orbiting satellites has high temporal resolution necessary for observing areas with frequent cloud cover. AVHRR allows monitoring of the seasonal changes of vegetation over large areas. This study was conducted to determine if the NDVI is useful for monitoring seasonal drought for evergreen tropical rainforests.

The study site is located in Ujung Kulon, a National Park located on the western coastal plain of Java, Indonesia. In order to determine the seasonal drought period and severity, a simple water balance model was developed for the area using monthly mean temperatures and total monthly precipitation for the years 1986-1988. FOREST-BGC was used to estimate the productivity of the study area for comparison with NDVI for two years, 1986 and 1987.

I found a significant positive correlation between the monthly NDVI and soil water availability, $r = 0.69$ for the year of 1987 (during an El Niño) and $r = 0.75$ for the year of 1988. A significant positive correlation between monthly NDVI and the current month precipitation was also found ($r = 0.68$) for 1986. Correlations between NDVI and the previous month's precipitation were significant; the correlation coefficients for 1986, 1987, and 1988 were 0.70, 0.51, and 0.85 respectively. High negative correlations between annually integrated NDVI and annually integrated soil moisture or precipitation indicated a possible effect of increased atmospheric water vapor and clouds (decreasing NDVI during wet years). A significant correlation between monthly NDVI and monthly net photosynthesis was found in 1987.

Climatic events such as an El Niño strongly control ecosystem processes of evergreen tropical rainforest in Indonesia by causing severe drought. NDVI can be used to monitor the length of the drought, possibly assisting in the estimation of forest fire potential.

ACKNOWLEDGEMENTS

I wish to express my sincere appreciation to my graduate advisor Dr. E. Raymond Hunt, Jr., for his continued support and encouragement on this project.

Special thanks must also be extended to committee members Dr. Steven Running, Dr. Stephen Siebert, and Dr. Darshan Kang for their guidance and direction.

I specially want to thank Mr. Muhammad Muchlis for providing me valuable data and information for the study site.

And finally, my deepest appreciation is expressed to my wife, Haryani Hidayat, for her patience and continued support throughout the length of this study.

TABLE OF CONTENTS

		Page
ABSTRACT		ii
ACKNOWLEDGEMENTS		iii
LIST OF TABLES		vi
LIST OF FIGURES		vii
LIST OF APPENDICES		viii
LIST OF ABBREVIATIONS		ix
CHAPTER		
I.	INTRODUCTION	1
	Background	1
	Objectives	2
II.	LITERATURE REVIEW	4
	NOAA Satellite Characteristics	4
	Vegetation Indices	5
	NDVI versus Productivity	7
	Water Balance	8
	El Niño	9
III.	STUDY AREA	10
	General Description	10
	Climate	10
	Soils	11
	Forest Types	12

IV. METHODS 15

Vegetation Index 15

Water Balance 16

FOREST-BGC 19

V. RESULTS AND DISCUSSION 21

Water Balance 21

Normalized Difference Vegetation Index . . . 22

Relationship between NDVI and Water Balance . 22

Integrated NDVI and Integrated Water Balance 32

Relationship between NDVI and Productivity . 32

Applications and Future Directions 34

VI. CONCLUSIONS 39

LITERATURE CITED 41

APPENDICES 45

LIST OF TABLES

Table Page

1. Characteristics of NOAA polar orbiting meteorological satellites 4

2. The AVHRR spectral channels, wavelengths and purposes 5

3. Mean Monthly Rainfall Data for Ujung Kulon 11

4. Soil Types and Geomorphological Units of Ujung Kulon 14

5. Regressions of monthly NDVI against monthly available water and precipitation for the three year observations 31

6. Regressions of monthly NDVI against monthly Photosynthesis 33

LIST OF FIGURES

Figure | Page

1. Temporal variation on monthly NDVI for Ujung Kulon (1986, 1987 and 1988) 24

2a. Comparison of monthly NDVI and soil moisture (available water), 1986 25

2b. Comparison of monthly NDVI and soil moisture (available water), 1987 26

2c. Comparison of monthly NDVI and soil moisture (available water), 1988 27

3a. Comparison of monthly NDVI and Precipitation (1986) 28

3b. Comparison of monthly NDVI and Precipitation (1987) 29

3c. Comparison of monthly NDVI and Precipitation (1988) 30

4a. Relationship of Annually Integrated NDVI and Annually Integrated Soil Moisture (1986-1990) 35

4b. Relationship of Annually Integrated NDVI and Annually Integrated Precipitation (1986-1990) 36

5a. Comparison of Monthly NDVI and Monthly PSN (1986) 37

5b. Comparison of Monthly NDVI and Monthly PSN (1987) 38

LIST OF APPENDICES

Appendix		Page
1.	The Climatic Water Balance for Ujung Kulon .	46
2.	Monthly Values of Heat Index Corresponding to Monthly Mean Temperature (°C)	49
3.	Soil Moisture Retention Table	50
4.	Geomorphological Map of Ujung Kulon	52
5.	Landscape Ecology Map of Ujung Kulon	53

LIST OF ABBREVIATIONS

AET	: Actual Evapotranspiration
APW	: Accumulation potential Water loss
AVHRR	: Advanced Very High Resolution Radiometer
CH1	: Channel 1 (Red wave band)
CH2	: Channel 2 (Near-infrared wave band)
D	: Deficit of water
ENSO	: El Niño Southern Oscillation
ET	: Evapotranspiration
FOREST-BGC	: Forest Bio Geochemical Cycles
GAC	: Global Area Coverage
GVI	: Global Vegetation Index
IFOV	: Instantaneous Field of View
LAC	: Local Area Coverage
MT-CLIM	: Mountain microclimate simulator
NDVI	: Normalized Difference Vegetation Index
NOAA	: National Oceanic and Atmospheric Administration
NPP	: Net Primary Production
P	: Precipitation
PE	: Potential Evapotranspiration
PSN	: Net Photosynthesis
Ro	: Water run off
S	: Surplus of water
ST	: Soil Water Storage (Available Water)
ΔST	: The change in soil moisture
UNDP	: United Nation Development Program

I. INTRODUCTION

Background

In 1982-1983, drought led to serious fires in the evergreen tropical rainforests of Indonesia. During that period of time, an estimated 3.5 million hectares of forests in the Indonesian province of East Kalimantan were damaged by drought and subsequent fires. Leighton et al. (1985) and Lennertz and Panzer (1984), reported by Malingreau et al. (1985), pointed out that preliminary estimates of damaged areas included : 800,000 hectares of primary lowland rainforests, 550,000 hectares of peat swamp forests, 1.2 million hectares of selectively logged forests and 750,000 hectares of shifting cultivation land. They estimated that the loss of standing timber and growing stock to be worth more than $ 5 billion. As a consequence, the Indonesian Government would like to develop early warning systems for forest fire danger.

The existing methods for drought monitoring depend on climatic data and ground-based observations. These methods, however, are time consuming and spatially restrictive. The limited ability to evaluate large areas using traditional techniques may be overcome through the application of remote sensing techniques.

Malingreau et al. (1985) demonstrated the use of the Advanced Very High Resolution Radiometer (AVHRR) on board the National Oceanic and Atmospheric Administration (NOAA) satellites for drought and fire detection in East Kalimantan (Indonesia) and Sabah (Malaysia). They found a decrease in the Normalized Difference Vegetation Index (NDVI) over large areas of tropical rainforests in Borneo (East Kalimantan and Sabah) that were partially destroyed by drought and fires. For the past ten years, Indonesia has invested heavily in remote sensing with the hope that the technology will help solve problems associated with natural resource management and environmental protection.

This study evaluates the potential of using AVHRR data to remotely sensed drought by analyzing the relationship between water balance and the satellite vegetation indices. By developing a simple, monthly water balance model, based primarily on climate data for the study site, information about seasonal drought and soil water availability can be compared to satellite NDVI.

Objectives

The first objective of this study was to investigate the application of AVHRR-NDVI data for monitoring seasonal drought of tropical evergreen rainforest in Indonesia. This was done by testing the relationship of monthly NDVI values and monthly water balance for the study area. My hypothesis was that there is a strong correlation between vegetation indices such as the NDVI and soil water availability. This hypothesis is based on the fact that the availability of soil moisture is one of the most important factors that determine plant growth. Available soil moisture was calculated from a monthly water balance because monthly total precipitation and mean air temperatures are generally available for the study site.

My second objective was to relate vegetation indices with net primary production (NPP), which can be estimated using the model FOREST-BGC (Running and Coughlan, 1988). Drought and low soil moisture are related to NPP and NDVI for temperate coniferous forest ecosystems (Running & Nemani, 1988). Thus, this objective extends knowledge on NPP and NDVI to tropical evergreen rainforest ecosystems.

II. LITERATURE REVIEW

NOAA Satellite Characteristics

The NOAA series of satellites was designed to operate in a near-polar sun-synchronous orbit at a nominal altitude of 833 km. The orbital period is 104 minutes, which results in 14.2 orbits per day. The NOAA satellite series has a payload of six instruments, including the AVHRR. NOAA attempts to maintain a two-satellite system that collects data in the morning and afternoon. This coverage provides an opportunity to acquire sufficient cloud-free data for most analyses (Miller et al., 1986). Table 1 shows the characteristics of NOAA meteorological satellites.

Table 1. Characteristics of NOAA polar orbiting meteorological satellites (Miller, et al., 1986)

PARAMETER	NOAA-6,8,10	NOAA-7,9
Inclination	98.7°	98.7°
Scan angle from nadir	± 55.4°	± 55.4°
IFOV at nadir (AVHRR)	1.1 km	1.1 km
Coverage	every 12 hrs	every 12 hrs
Equatorial Crossing	7:30 am	2:30 pm

The AVHRR, which has been carried by NOAA series of satellites since 1979, is a cross-tract spin-scan radiometer with a scan rate of 360 rotations per minute. It records data within an angle of ± 55.4° from nadir, equivalent to a swath width of 2600 km. Data are digitized on board the spacecraft at a rate of 2048 samples per scan per channel (Kidwell, 1984). The AVHRR provides five spectral channels : one visible, one near-infrared, and three thermal (Matson and Holben, 1987; Drury, 1990). Table 2 illustrates the five channels of AVHRR including the wavelength and the purposes.

Table 2. The AVHRR spectral channels,wavelengths and purposes (Lillesand and Kiefer, 1987)

Channel No.	Wavelength (μm)	Purpose
1.	0.58 - 0.68	Daytime cloud, snow,and ice mapping.
2.	0.725 - 1.10	Surface water delineation, vegetation assessments.
3.	3.55 - 3.93	Nighttime cloud mapping, sea surface temperature, land/water distinction, hot spot detection (forest fire, volcanic activity).
4.	10.30 - 11.30	Day/night cloud mapping, sea and land surface temperaturemeasurements, soil moisture and volcanic eruptions.
5.	11.50 - 12.50	Sea and land surface temperature measurements and soil moisture

Vegetation Indices

Vegetation indices such as the NDVI derived from NOAA-AVHRR data have been utilized by researchers to monitor seasonal changes of plant greenness (Justice et al., 1985) and to classify land cover types (Tucker et al., 1985; Townshend et al.,1987). NDVI is an effective tool for monitoring the condition of vegetation (D'Iorio et al., 1989).

As a quantitative measure which represent biomass or vegetative vigor, increased NDVI values indicate increased active, green biomass. However, Burgan et al.(1990) examined various problems that can produce unwanted reductions in the NDVI. The amount of atmosphere between the observation site and the satellite is one potential problem. As satellite viewing angle moves off the vertical, the amount of reflected light reaching the AVHRR sensor is reduced because the reflected light must travel through more atmosphere. Also, reduction in the transmissivity of the atmosphere by water vapor, smoke, and clouds reduces the amount of reflected light reaching the sensor.

Justice et al. (1991) investigated the effect of water vapor on the normalized difference vegetation index for the Sahelian region. They found that increases in atmospheric water vapor within the Sahel resulted in a reduction of the NDVI values.

The potential of using AVHRR data, which have high temporal and coarse spatial resolution, has been demonstrated by Tucker et al. (1985 and 1986), Townshend and Justice (1986), and Justice et al. (1986). They evaluated the utility of AVHRR-NDVI data for monitoring vegetation condition in Africa, and found that the NDVI values are closely correlated to photosynthetic activity of vegetation.

Henricksen and Durkin (1986) found a strong correlation between rates of change of the NDVI calculated from AVHRR data and threshold values of soil moisture index at the beginning and ends of growing periods. They used this approach in order to determine growing period in Africa and to develop a model for drought early warning from space.

Through an analysis of anomalies in the development of selected vegetation formations, Malingreau (1986) evaluated the impact of the 1982-1983 El Niño Southern Oscillation (ENSO) using the global vegetation index, GVI (NDVI at 4-km resolution). ENSO causes warming of the Pacific waters which in turn causes severe drought in Southeast Asia (Malingreau et al., 1985).

NDVI versus Productivity

The relationship between the AVHRR data and net primary productivity for various North American biomes has been investigated by Goward et al. (1985) and Goward et al. (1987). They found that annually integrated patterns of NDVI closely correspond to the patterns of net primary production of the North and South American continents.

Running and Nemani (1988) and Running (1990) demonstrated the use of AVHRR-NDVI for estimating the terrestrial net primary production. They found a strong correlation between annual integrated NDVI and annual photosynthesis, transpiration, and net primary production for seven sites of contrasting climate in North America.

Prince (1991) examined the relationship between multi-temporal sums of vegetation indices derived from NOAA-AVHRR and primary production in semi arid grassland in three Sahelian countries over a period of 8 years (1981-1988). His study results indicated that there is a strong linear relationship between seasonal production and integration of AVHRR-NDVI data.

Water Balance

Soil water balance is a tool to describe the relationship between inflow and outflow of water within circulation process in a certain area and in a certain period. Hillel (1971) defines soil water balance as a detailed budget of the gains and losses of water, and the change of soil moisture storage over a certain period.

The climatic water balance was introduced by Thornthwaite and Mather (1957). They developed a monthly and a daily water balance model using a bookkeeping technique. Frere and Popov [1979; quoted by Oldeman and Frere (1982)], define water balance as the difference between water supply (precipitation) and potential water loss (potential evapotranspiration). In a simple form, the equation of water balance given by Hillel (1971) is :

$$W\_in - W\_out = \Delta W \quad (1)$$

where W_in is the amount of water added; W_out is the amount of water withdrawn over a certain period; and ΔW is the change in soil water content during the same period. When W_in > W_out, ΔW is positive; conversely, when W_out > W_in, ΔW is negative.

El Niño

For more than a century El Niño, the Spanish term for Christ child, has been applied by fishermen to the annual appearance at Christmas time of warm water off the coast of Ecuador and northern Peru. This anomalous warming of the sea surface in the equatorial Pacific is associated with a vast fluctuation in atmospheric pressure. El Niño events with anomalous warming of the tropical ocean have occurred at several-year intervals since before written records began (Enfield, 1989).

El Niño of 1982-1983 created drought in parts of Indonesia, the Philippines and Papua New Guinea, and had serious impact upon the agricultural production (Malingreau et al., 1985). Monastersky (1991) states that the last El Niño occurred from late 1986 through 1987. This seasonal event causes floods in some regions (such as California) and drought in others (such as Indonesia).

III. STUDY AREA

General Description

The study area is located in Ujung Kulon, Indonesia. The National Park Ujung Kulon, occupies a peninsula between 6° 38' and 6°52' south latitude and 105°12' and 105°30' east latitude. It is located on the south-western end of Java and is almost completely separated from Java island by the Welcome Bay (Appendix 5).

In 1921, the Ujung Kulon peninsula became a strict nature reserve. In 1937, the reserve status was changed into a private hunting reserve. The status was changed back to a nature reserve in 1958, and finally in 1980, it was declared as a National Park [Hommel, 1983, in Anonymous, (1985)].

Climate

Ujung Kulon has a seasonal perhumid climate. The climatic data (rainfall) shows that the wet months are from December to April and the dry months are from May to September. Using Mohr's index (Whitmore, 1985) such rainfall pattern can be classified as rainfall type C. Mohr's index is expressed as a ratio :

$$Q = \frac{\text{dry months}}{\text{wet months}}$$

The Q value indicates the rainfall type of the study area based on the following categories :

Type A, Q = 0 - 14.3 : perhumid

Type B, Q = 14.3 - 33.3 : slightly seasonal

Type C and D, Q = 33.3 - 100 : seasonal

Type E and F, Q = 100 - 300 : strongly seasonal.

The average temperature ranges from 25-30°C, with humidity of 80-90 percent. Table 3 illustrates mean monthly rainfall data for Ujung Kulon.

Table 3. Mean Monthly Rainfall Data for Ujung Kulon (mm).

Jan.	Feb.	Mar.	Apr.	May.	Jun.	Jul.	Aug.	Sep.	Oct.	Nov.	Dec.	
450	342	301	257	163	114	150	186	122	206	330	466	a
443	377	325	258	171	178	130	138	141	263	351	474	b

Source : Anonymous, (1985).
a - Based on 14 years (1886-1900).
b - Based on 40 years (years not given).

Soils

The various soils on mountains and plateaus are covered with layer of volcanic ash originating from Krakatau eruption of 1883. The amount of ash deposited varies from place to place. Table 4 describes the soil types and geomorphological units of Ujung Kulon. Appendix 4 illustrates the geomorphological map of Ujung Kulon.

Forest Types

In general, the forest types in Ujung Kulon can be classified as follows (Anonymous, 1985) :

1. *High-elevation Forests.* This type occur at elevation higher than 150 m above mean sea level, and could be found on ridges or slopes. The extent of this forest type was estimated as 3,222 hectares (18.4 % of the study area).

2. *Low-elevation Forests.* This appear on flat to undulating or undulating to rolling terrain in areas below 150 m above mean sea level. Forests on undulating to rolling terrain with an open canopy covers an extent of 666 (3.8 % of the study area) ha and the one with a dense canopy, 3,501 ha (20 %). Open canopy forests on flat to undulating terrain is the major forest type found in this area and its extent was estimated as 4,752 ha (27 %). The similar type with a dense canopy occupies 2,736 ha (15.5 % of the study area).

3. *Coastal Forests.* Mangroves cover an extent of 720 ha. and beach forests occur on coral sediments near the shores covering 963 ha (5.5 %). Also, coastal forests could be detected adjoining sandy shores or on coastal ridges occupies 468 ha (3.4 % of the study area).

4. *Shrublands.* This consists of shrub vegetation occasionally in association with larger trees.

5. *Grasslands.* This area is covered by dry grasslands and Swampy grasslands.

Appendix 5 illustrates the spatial arrangement of forest and vegetation types in Ujung Kulon.

Since 1946 the last vast areas of alang-alang savannah (shrublands) have disappeared. At present these areas are covered by the specific, very homogeneous forest type, dominated by *Ardisia- Buchanania* (coastal forest). Further succession is believed to lead to very slowly towards a more mature form of *Ardisia-Buchanania* forest or a *Syzygium polyanthum* forest. The pattern of former fields in the interior can still be more or less recognized. Instead of being covered by forest again, they turned into extensive rattan-shrublands (*Camalus-Amomum* community). Succession towards more woodlike vegetation is very slow, perhaps leading to either a *Drypetes-Bambusa* (low-elevation) forest or an *Arenga obtusifolia* (high-elevation or low-elevation) forest [Hommel, 1983 (in Anonymous, 1985)].

Table 4. Soil Type and Geomorphological Units of Ujung Kulon.

Geomorphological Units	Soil Type
1. Mountain & hills	
1a. Payung mountain range	Clay, Sandy Loams and Loams
1b. Western hills	Clay and Clay Loams
2. Structural plateau	
2a. Upper level	Clay
2b. Middle level	Clay
2c. Lower level	Gravelly Clay and Clay Loams
3. Beach ridge	Sandy Clay Loams
4. Plains	
4a. Erosional plains	Clay
4b. Alluvial plains	Gravelly Clay and Clay Loams
4c. Coastal plains	Clay, Clay Loams and Loams
5. Bottom lands	Clay
6. Tidal swamps	Clay

Source : Anonymous, 1985.

IV. METHODS

Vegetation Index

Generally, there are two products of AVHRR available : local area coverage (LAC) and global area coverage (GAC) data. LAC data have a pixel size of view of 1.1 km, whereas GAC data, which are produced on a daily basis for the whole globe, have 4 km resolution. In this study, the monthly NDVI were selected from weekly-composited global vegetation index (GVI) by taking the highest value of NDVI for the month. The data are provided by the Indonesian Remote Sensing Center, as a result of joint research project between Indonesian Government and the United Nation Development Program (UNDP).

NDVI is calculated by dividing the difference between channel 2 and channel 1 of AVHRR data by their sum :

$$\mathbf{NDVI = (CH2 - CH1)/(CH1 + CH2)} \quad (2)$$

where NDVI is Normalized Difference Vegetation Index, CH1 and CH2 are digital numbers of channels 1 (red wave band) and 2 (near-infrared wave band) of NOAA-AVHRR sensor (see Table 2).

A comprehensive integrated microcomputer software system, MICVEGI2 was used to calculate NDVI time series data. The system was designed to be used on IBM or IBM compatible micro computer. As an integrated system, MICVEGI2 contains various functions to :

1. Define Locations
2. Define Polygons

3. Define five time periods of NDVI data
4. Extract scaled NDVI data from the GVI satellite files
5. Smooth NDVI time-series data
6. Download NDVI for input to Spread Sheet Software
7. Display NDVI data
8. Print NDVI data.

Water Balance

The climatic water balance equation given by Thornthwaite and Mather (1957) is :

$$\mathbf{P = ET + \Delta ST + Ro} \quad (3)$$

where P is precipitation; ET is evapotranspiration; ΔS is the change in soil moisture; and Ro is water run off. In order to compute the climatic water balance at a certain area, mean monthly or daily air temperatures, mean monthly or daily precipitation, conversion and computational tables, water holding capacity of the depth of the soil are necessary.

The climatic water balance model for Ujung Kulon was developed based on climatological data from 1986 through 1990. For this study, I concentrated on 1986, 1987 and 1988 because 1987 represents a dry year (caused by an El Niño), 1986 represents an abnormally wet year, and 1988 represents an average year. Monthly precipitation and mean monthly air temperature data of the study area were obtained from the Indonesian Meteorological and Geophysical Agency.

Potential Evapotranspiration. Potential evapotranspiration (PE) is the potential water loss from a large homogeneous, vegetation-covered area that never suffers from a lack of water. Potential evapotranspiration is primarily a function of climatic conditions, such as air temperature, and is not a function of type of vegetation, type of soil, soil moisture content, or land management practices (Mather and Rowe, 1979).

There are several methods for estimating evapotranspiration. For example, Blaney and Cridle [in Schwab et al., 1981)] developed a method for determining evapotranspiration from climatological and irrigation data. To estimate the evapotranspiration from the study area, the following empirical equation given by Mather and Rodriquez (1979) was used :

$$E = 16\ (10t/I)^{A} \qquad (4)$$

where E is monthly potential water loss (potential evapotranspiration); t is mean monthly air temperature in°C; and I is annual heat index. The exponent, A, is calculated from :

$$A = 6.75\times10^{-7}\ I^{3} - 7.71\times10^{-5} I^{2} + 1.792\times10^{-2} I + 0.49239 \qquad (5)$$

The value of I is the sum of the 12 monthly heat indices (i), which are obtained from the following formula :

$$i = (t/5)^{1.514} \qquad (6)$$

Actual Evapotranspiration. Actual evapotranspiration (the actual water loss from a vegetated area) depends on type of vegetation, type of soil, soil moisture content, or land management practices in addition to the climatic factors (Thornthwaite and Mather, 1955). Actual evapotranspiration is equal to potential evapotranspiration whenever precipitation is greater than potential evapotranspiration. When P-PE is negative, actual evapotranspiration equals precipitation for the month plus the change in soil moisture storage.

Soil Moisture Storage. Many investigators have considered the way in which water is removed from soil storage by plants. Most assume that when the soil is at field capacity, the roots will be able to remove water easily. However, as the soil begin to dry, it becomes increasingly difficult for the plants to obtain all the water that is needed (Mather, 1979). Thornthwaite and Mather (1955) have suggested that when the soil moisture is at 75 percent of field capacity, the plants will be able to obtain 75 percent of the necessary water not supplied by precipitation.

Soil moisture can increase to maximum storage when P - PE is positive. In the bookkeeping procedure, Thornthwaite and Mather (1957) assumed that precipitation is used first for potential evapotranspiration, second added to storage in the soil, and finally additional water above the maximum storage is treated as runoff. In this study, maximum soil moisture was set equal to the soil available water, which was measured to be 150 mm per meter depth (Supraptohardjo et al., 1966).

Moisture deficit is the difference between potential and actual evapotranspiration month by month. Moisture surplus is the excess P-PE whenever soil moisture is at the maximum storage. Thus, there is no deficit of water when P-PE is positive; when P-PE is negative there can be no surplus of water. However, moisture surplus does not always occur when P-PE is positive, for as long as soil moisture storage is below the available water, no surplus can develop (Mather, 1979). On the other hand, moisture deficit does not always occur when P-PE negative. It depends on the actual evapotranspiration. As long as potential evapotranspiration does not exceed actual evapotranspiration there will be no deficit of water. Water runoff is only about 50 percent of the surplus water (Thornthwaite & Mather, 1957).

FOREST-BGC

FOREST-BGC (Bio Geochemical Cycles) is an ecosystem process simulation model that calculates the carbon, water and nitrogen cycles through forest ecosystems (Running and Coughlan, 1988). FOREST-BGC, requires daily meteorological data, such as maximum and minimum air temperatures, dew point temperature, total shortwave solar radiation and precipitation (Running and Nemani, 1988 ; Hunt et al., 1991).

The model calculates canopy interception and evaporation, transpiration, photosynthesis, growth and maintenance respiration, carbon allocation above and below-ground, litterfall, decomposition and nitrogen mineralization.

Daily and monthly precipitation, maximum and minimum air temperature data from Serang and Cigeulis Meteorological Station for the year of 1986 and 1987 were used as inputs to the model as these were the only years with daily data available. The mountain microclimate simulator, MT-CLIM (Running et al. 1987), was used to produce site specific conditions, such as daily solar radiation and dew point temperature, by extrapolating base station data.

FOREST-BGC was parameterized from published data on tropical rainforest. Biomass, specific leaf area and leaf area index for a mature tropical rainforest in Malaysia were obtained from Cannell, 1982. Leaf nitrogen concetration and photosynthetic rate data for a tropical rainforest in New Britain were obtained from Mooney et al., (1984).

V. RESULTS AND DISCUSSION

Water Balance

Appendix 1 illustrates the climatic water balance for 1986 through 1990 at Ujung Kulon. Monthly potential evapotranspiration based on Thornthwaite's empirical equation (4) was found to vary from a value of 114 mm in February 1989 to the highest value of 161 mm in October and November 1987.

Monthly precipitation and potential evapotranspiration did not coincide in 1986, 1987 and 1988. Generally there was too much precipitation in the wet season leading to runoff, and not enough during the dry season. Subtracting potential evapotranspiration from the values of precipitation (P-PE) results in a series of positive and negative values (Appendix 1).

In 1987, estimated moisture deficit occurred earlier than in 1988. In 1987, total moisture deficit was 616 mm (over 7 months), whereas in 1988, total moisture deficit was 228 mm (over 5 months), and in 1986 total moisture deficit was 187 (over 6 months). This means that in the case of total moisture deficit and the length of moisture deficit period, 1987 was the year with longest dry season, which was caused by an El Niño.

Normalized Difference Vegetation Index

Maximum NDVI values for Ujung Kulon were selected for each month from the 1986,1987 and 1988 GVI data set. The general pattern of the NDVI values for the three years observation at Ujung Kulon, shows that the values dropped at the beginning of the dry period in June (Figure 1). Seasonal values of the NDVI during the wet season (January trough April) 1987 were less compared to 1986 and 1988. During the dry season (June through October) the NDVI values of 1987 were greater than either 1986 or 1988 (Figure 1).

The drier conditions in 1987 may have caused greater transmittance in the near infrared channel thereby increasing NDVI. The wavelength region of this band contains some water vapor absorption features (Gao and Goetz, 1990). Justice et al. (1991) reported that in extreme cases the atmospheric water vapor can reduce the NDVI by 0.1 in the Sahelian regions of Africa.

Relationship between NDVI and Water Balance

NDVI curves for three years of observations (1986,1987, and 1988) decreased with lower soil moisture (Figure 2). The monthly NDVI decreased during dry season correlated with the decrease in soil moisture. The estimated range in monthly soil moisture during 1987 was from 150 mm during the wet season to 1 mm during the dry season, whereas the NDVI values ranged from 0.6 to 0.23 (Figure 2b).

In the case of 1988 during the dry season, the monthly NDVI values also followed the pattern of soil moisture. The NDVI increased in November 1988 due to the increased in soil moisture. In 1986, this phenomenon was slightly different (Figure 2a). The dry season started in March which was indicated by a decreased in soil moisture and followed by a decreased in NDVI. The soil moisture increased again in July and followed by an increased in NDVI value.

The change of NDVI over time showed the similar patterns with the precipitation patterns (Figure 3). Decreases and increases in NDVI corresponded to decreases and increases in precipitation, respectively. Table 5 shows the linear regressions between NDVI and soil water availability, previous and current precipitation. The variability in the correlation between NDVI and the current month precipitation range from r = 0.49 in 1987 to r = 0.68 in 1988. The correlation between NDVI and the previous month's precipitation ranged from r = 0.51 to 0.85 (Table 5). These show that the monthly NDVI data were more linearly related to previous month's precipitation compare to the current month's precipitation.

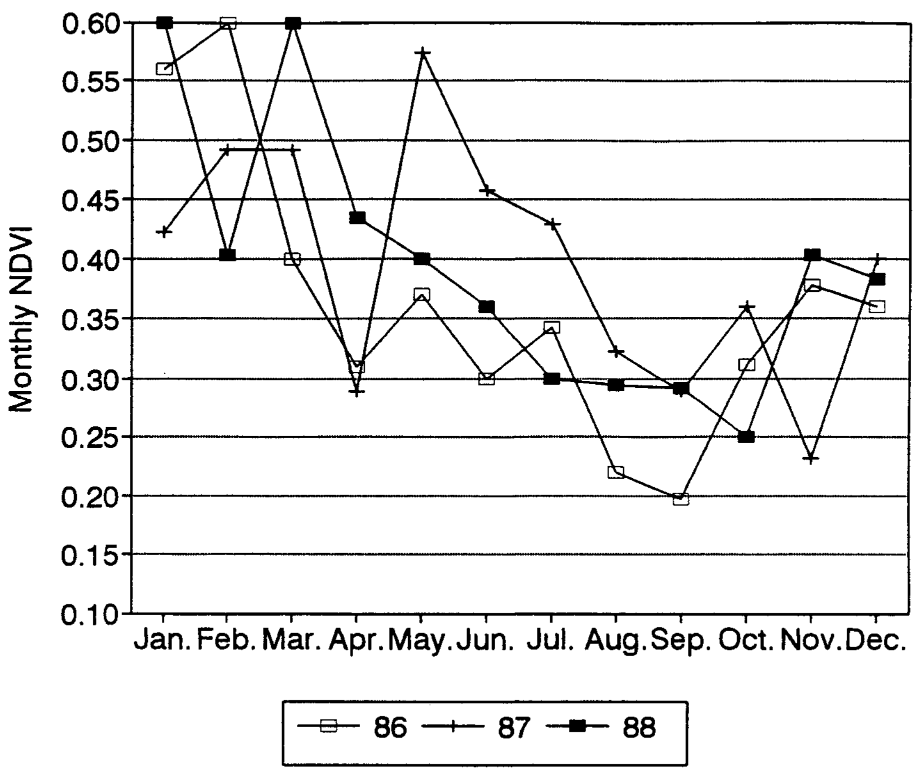

Figure 1. Temporal variation of monthly NDVI for Ujung Kulon (1986, 1987 and 1988)

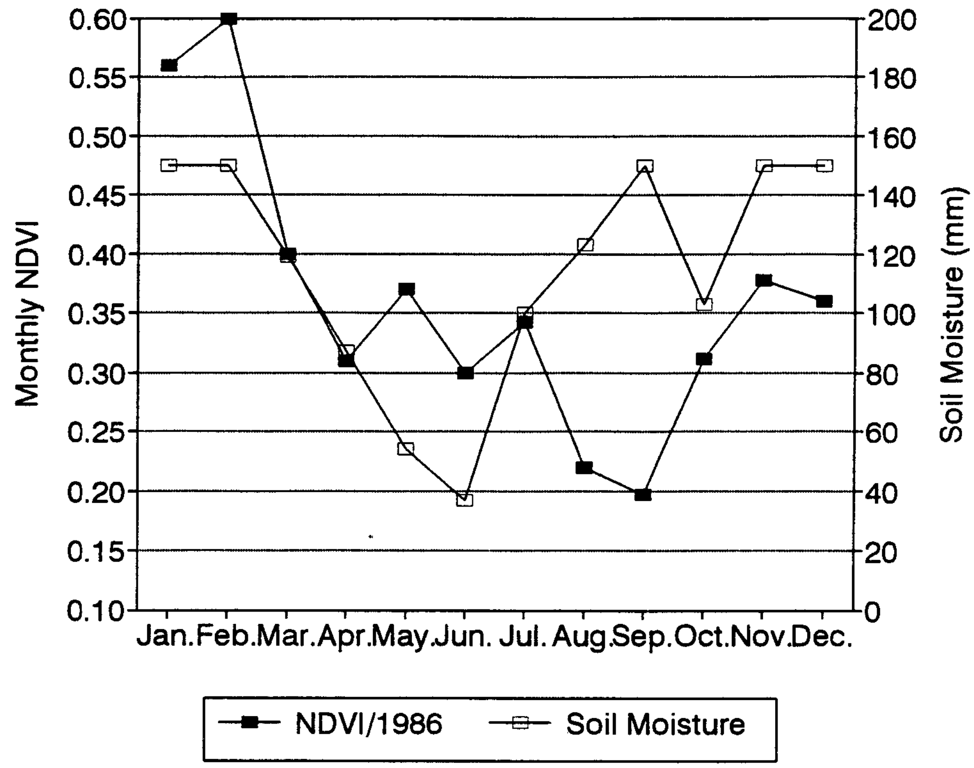

Figure 2a. Comparison of monthly NDVI and soil moisture (available water) (1986).

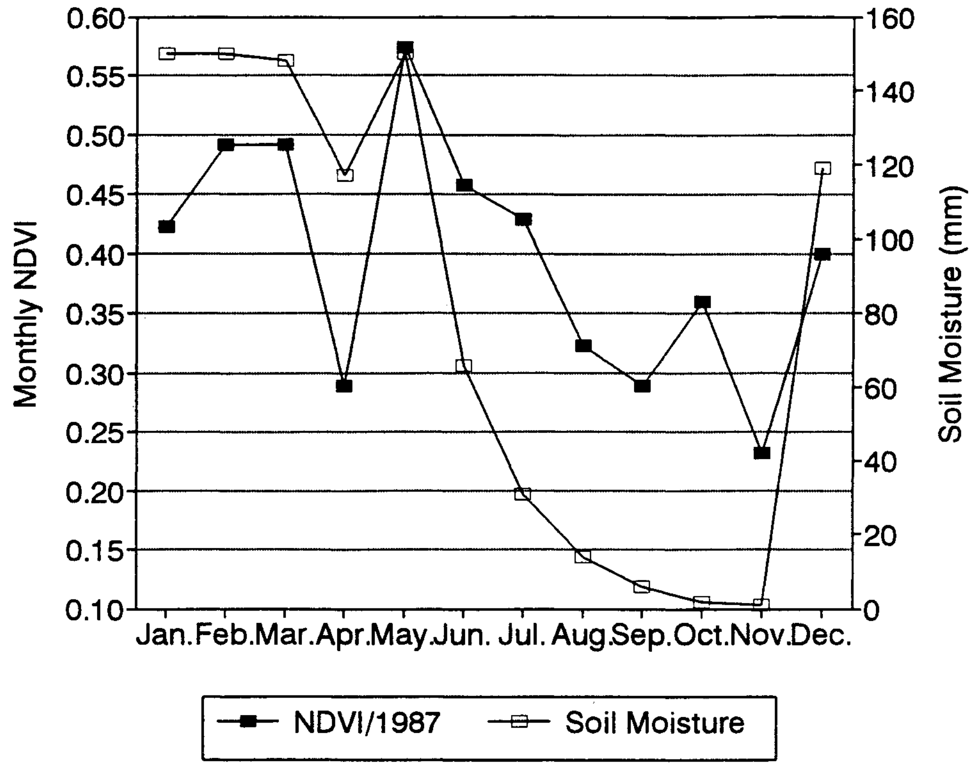

Figure 2b. Comparison of monthly NDVI and soil moisture (available water) (1987).

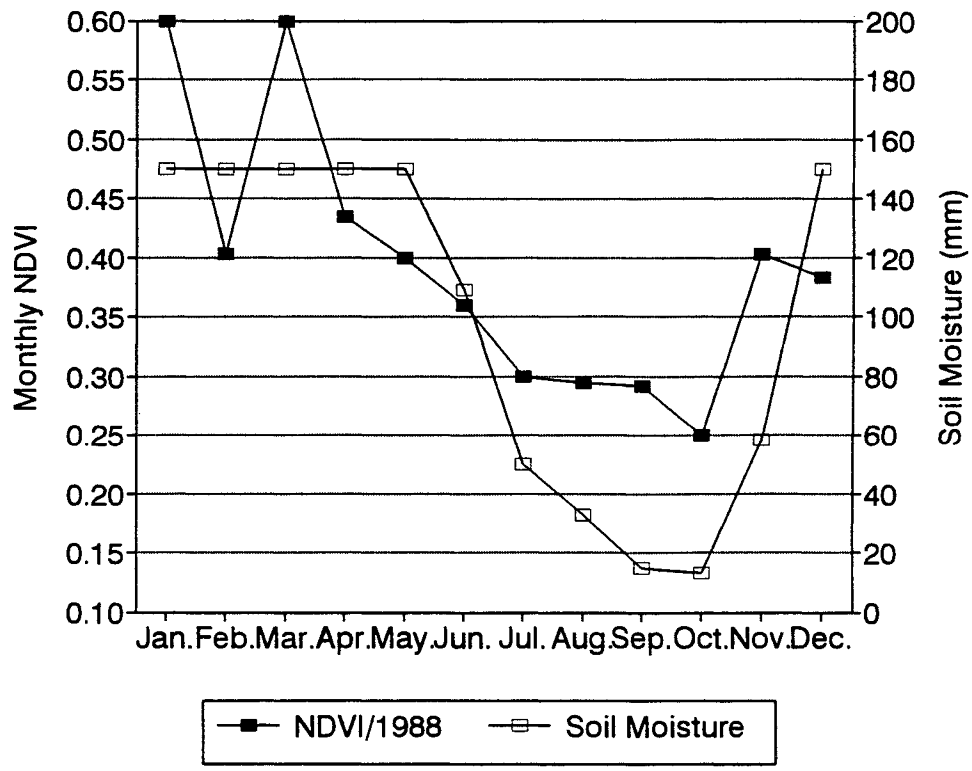

Figure 2c. Comparison of monthly NDVI and soil moisture (available water) (1988).

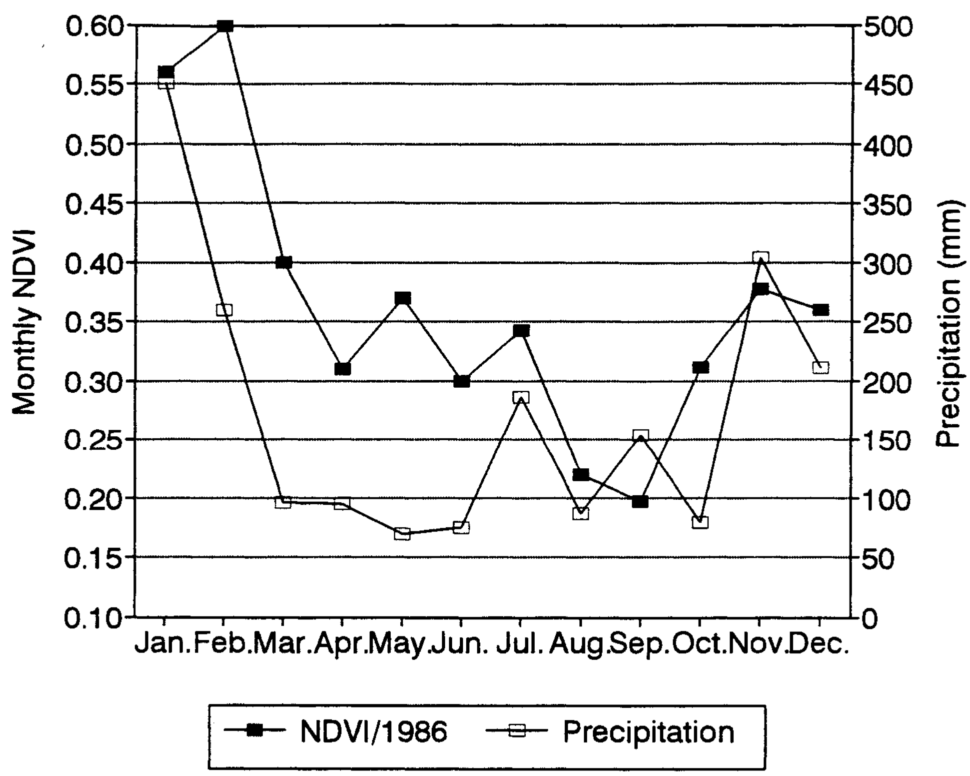

Figure 3a. Comparison of monthly NDVI and precipitation (1986).

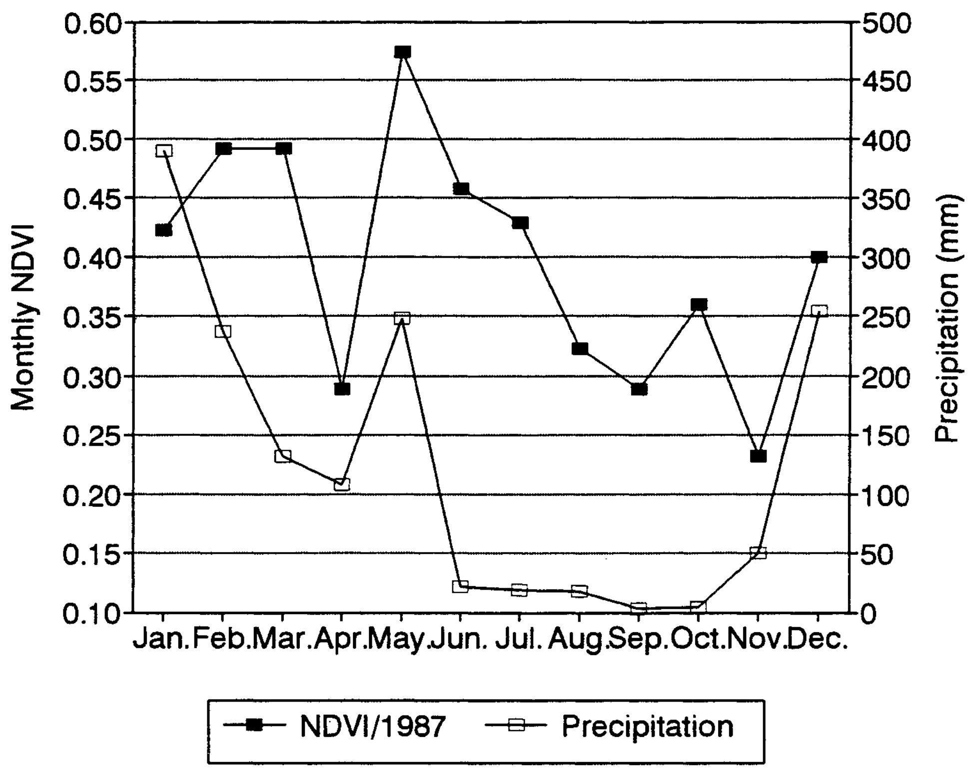

Figure 3b. Comparison of monthly NDVI and precipitation (1987).

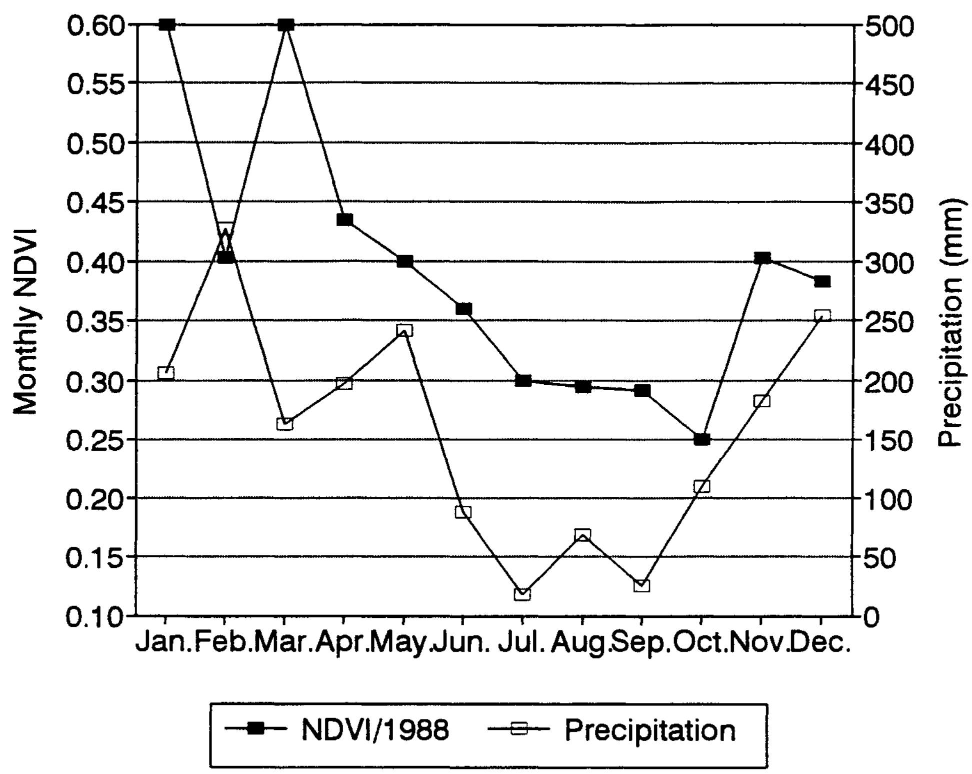

Figure 3c. Comparison of monthly NDVI and precipitation (1988).

Table 5. Regressions of monthly NDVI against monthly available water and precipitation for the three years observations.

Year	Equations[a]	r	P[b]
1986	NDVI = 0.000913 ST + 0.257915	0.30	0.8318
	NDVI = 0.000 681 P(t) + 0.245155	0.68	0.9922
	NDVI = 0.000603 P(t-1) + 0.240703	0.70	0.9948
1987	NDVI = 0.001061 ST + 0.31205	0.69	0.9931
	NDVI = 0.000386 P(t) + 0.348655	0.49	0.9479
	NDVI = 0.000402 P(t-1) + 0.34063	0.51	0.9551
1988	NDVI = 0.001418 ST + 0.253976	0.75	0.9975
	NDVI = 0.000576 P(t) + 0.302922	0.50	0.9490
	NDVI = 0.00099 P(t-1) + 0.238114	0.85	0.9998

a. Independent variables : ST = Soil Moisture Storage (available water); P(t) = Current month's precipitation; P(t-1) = Previous month's precipitation.
b. P : Probability of significance

Integrated NDVI and Integrated Water Balance

In order to investigate the general correspondence between NDVI and the water balance, the relationship of integrated NDVI and yearly precipitation and available water were also tested (Figure 4). The tests were performed based on five years of observation (1986-1990).

Interestingly, instead of the hypothesized positive correlations between NDVI and water balance, significant negative correlations were obtained(Figure 4). The linear regression equations are : NDVI = -0.00062P + 5.709196 (r = -0.79, p = 0.9477) and NDVI = - 0.00095ST + 5.722548 (r = -0.89, p = 0.9819). These equations indicate that the dryer years had the higher NDVI values. One possible explanation may be that during dry years the atmosphere had less water vapor and clouds, thereby increased atmospheric transmissivity in the infrared band thereby increasing NDVI (Justice et al., 1991). Another possible reason for the negative correlation may be the growth of the plants during the dry periods was controlled by phenology rather than water balance (D'Iorio et al., 1989).

Relationship between NDVI and Productivity

Monthly NDVI data were plotted against monthly net photosynthesis for 1986 (before the EL Niño) and 1987 (during the EL Niño). A significant correlation between monthly vegetation indices and monthly photosynthesis was found in 1987 (Figure 5). In the case of 1986, the correlation between monthly NDVI and monthly net photosynthesis was not significant. Negative values of monthly photosynthesis during dry periods (Figure 5), resulted from water stress, which closed the stomata and inhibited photosynthesis, however the foliage was still respiring. Table 6 shows the correlations between monthly NDVI and monthly PSN.

In 1986, simulated net primary production (NPP = PSN - total respiration) was 38.632 Mg C ha^{-1} $year^{-1}$, whereas in 1987, NPP was 21.248 Mg C ha^{-1} $year^{-1}$. Average NPP for the two years was 29.94 Mg C ha^{-1} $year^{-1}$, which is very close to the measured NPP, 26.90 Mg C ha^{-1} $year^{-1}$, for a similar tropical rainforest in Malaysia (Cannel, 1982).

Table 6. Regressions of monthly NDVI against monthly Photosynthesis

Year	Equations[a]	r	P[b]
1986	PSN = 7216.575 NDVI + 2225.934	0.36	0.8742
1987	PSN = 26046.5 NDVI - 7662.91	0.66	0.9910

a: Variables : PSN = monthly photosynthesis (Mg carbon ha^{-1} $month^{-1}$); NDVI = monthly composited vegetation indices (unitless).
b: P = Probability of significance

Application and Future Directions

By taking into account the effect of cloud and atmospheric water vapor on NDVI values this approach has potential implications for drought monitoring for areas with high cloud cover such as Sumatera and Sulawesi. Justice et al. (1991) and Eck and Kalb (1991) proposed methods for atmospheric water vapor and cloud correction. In addition, local area coverage (LAC) will be used in the future to obtain higher resolution in order to separate NDVI of the different vegetation types (Appendix 5).

For regions with pronounced dry seasons such as eastern part of Indonesia, this approach seems to be very useful for monitoring drought from space. Drought can be related to forest fire potential. However, without an atmospherically corrected NDVI, the severity of drought may not be determined (Figure 4)

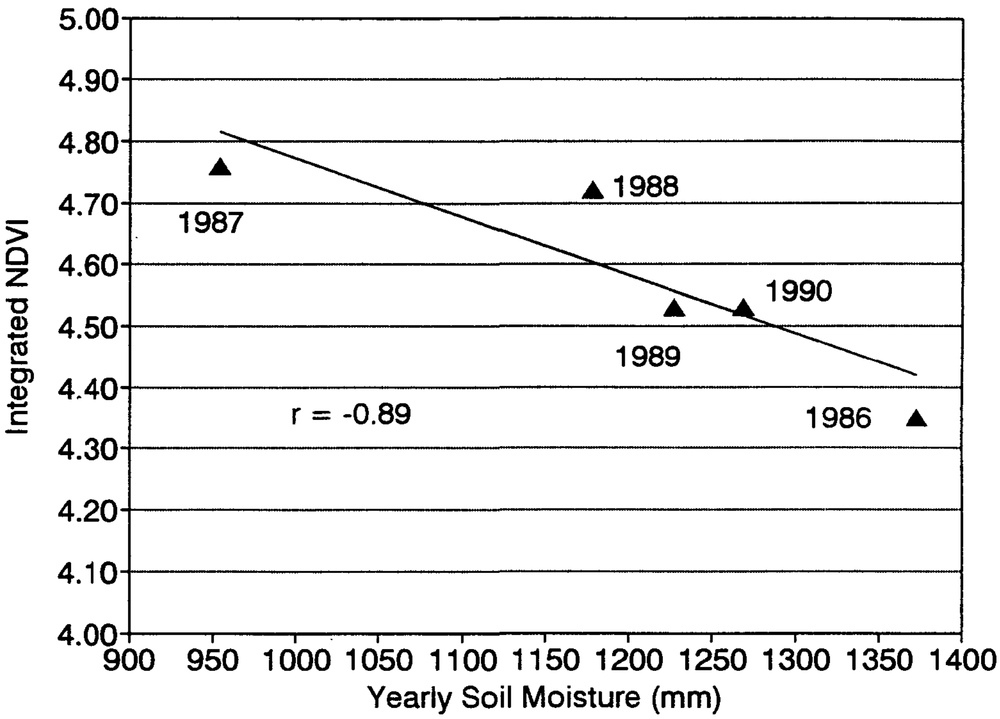

Figure 4a. Relationship of Annually Integrated NDVI and Annually Integrated Soil Moisture (1986-1990)

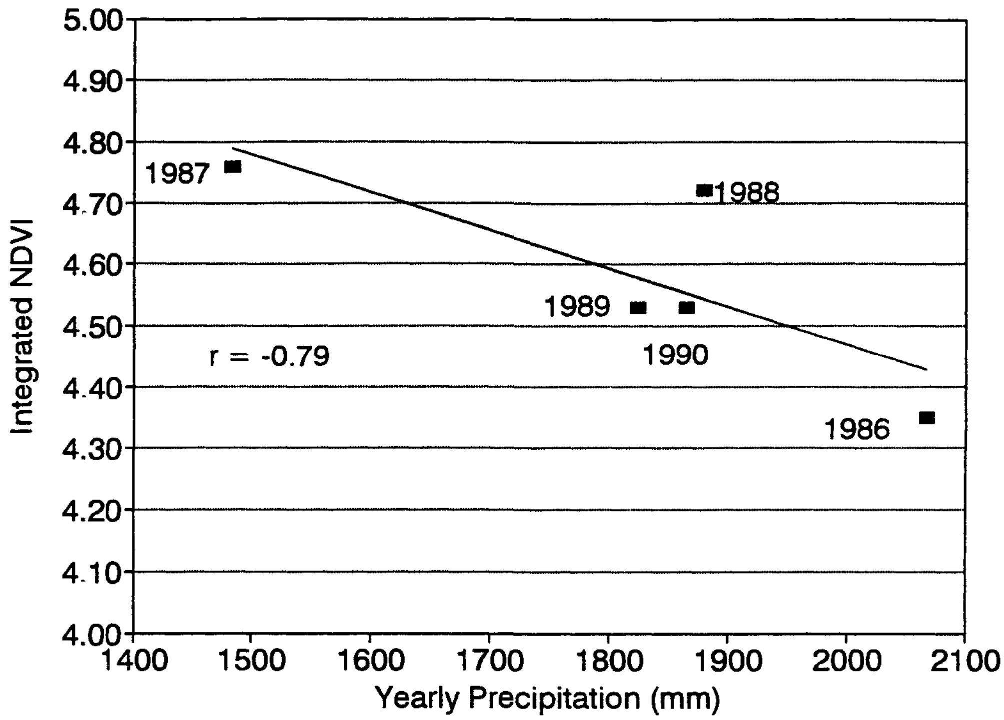

Figure 4b. Relationship of Annually Integrated NDVI and Annually Integrated Precipitation (1986-1990)

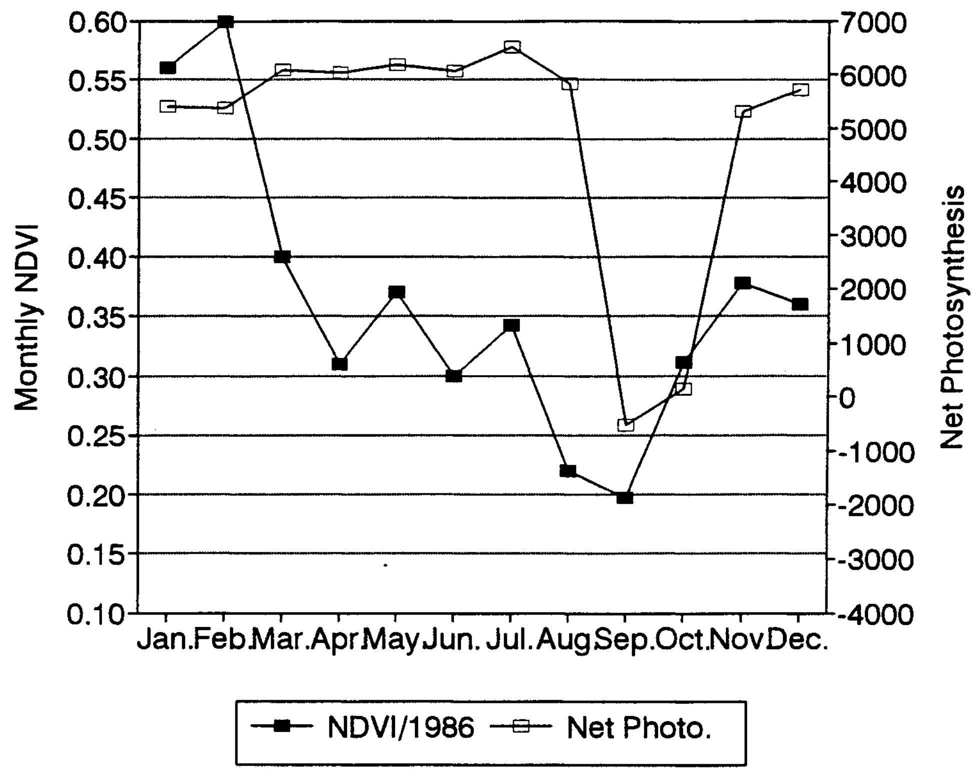

Figure 5a. Comparison of monthly NDVI and monthly PSN (1986)

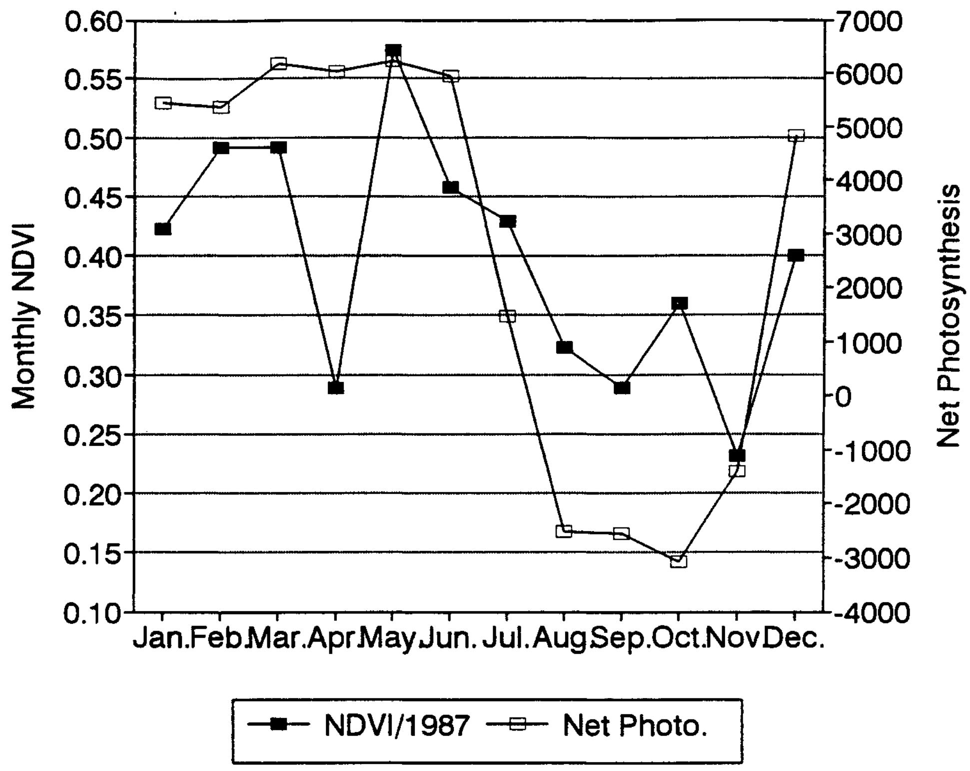

Figure 5b. Comparison of monthly NDVI and monthly PSN (1987)

VI. CONCLUSIONS

I found that for 1986, the NDVI of Ujung Kulon was more closely related to precipitation (both current and previous month) than soil moisture. During the El Niño (1987), NDVI and plant growth in Ujung Kulon was more correlated with soil water availability than precipitation. From the climatic water balance it was shown that 1987 was the driest year due to the El Niño effect. The NDVI seems most closely related to precipitation of the previous month, with 1988 (after the EL Niño) exhibiting the strongest correlation.

I also found that there were strong negative relationships between annually integrated NDVI and annually integrated precipitation (r = 0.79) and annually integrated available soil water (r = 0.89). I suggest, following Justice et al., (1991), that due to cloud or atmospheric water vapor effects, the NDVI values during the wet years were less than during the dry years.

A significant positive correlation between monthly vegetation indices and monthly photosynthesis was found during the El Niño (1987). Thus, monthly NDVI data may be useful as a predictor for changes in monthly photosynthesis but not annual photosynthesis.

The monthly NDVI values based on the GVI data apparently are reliable to determine the length of seasonal drought in the tropical evergreen rainforest in Indonesia. However, the negative correlations of integrated NDVI with annual water balance show that the severity of the drought can not be determined without atmospheric correction.

This research is directed to remotely sensing drought because during drought fires could destroy large areas of forests. The existing methods for drought monitoring are time consuming and spatially restrictive. Consequently, the use of remotely sensed data for drought early warning is an attractive proposition, however, more research in this area needs to be done.

VII. LITERATURE CITED

Anonymous, 1985. An Approach to Identify and Map Vegetation Types in Ujung Kulon National Park, West Java, Indonesia, Using Remote Sensing Techniques. ESCAP-BIOTROP Training Course Report, 4 November - 13 December 1985, Bogor, Indonesia.

Burgan, R.E., Roberta A.H., J. Eidenshink, and L. Werth. 1990. AVHRR Estimation of Vegetation Greenness and Site Moisture (unpublished reference).

Cannell, M.G.R. 1982. World Forest Biomass and Primary Production Data. Academic Press, New York.

D'Iorio, M.A., J. Cihlar, and L. St-Laurent. 1989. Relationship between AVHRR-NDVI and Environmental Parameters, in Proceedings : IGARSS'89/12th Canadian Symposium on Remote Sensing, Vancouver : 1326-1330.

Drury, S.A. 1990. A Guide to Remote Sensing, Interpreting Images of the Earth. Oxford University Press, New York.

Eck, T.F. and V.L. Kalb. 1991. Cloud-screening for Africa using a geographically and seasonally variable infrared threshold. Int. J. Remote Sensing, 12(6): 1205-1221.

Enfield, D.B. 1989. El Niño, Past and Present. Reviews of Geography, 27(1): 159-187.

Gao, B.-C. and A.F.H. Goetz. 1990. Column Atmospheric Water Vapor and Vegetation Liquid Water Retrievals From Airborne Imaging Spectrometer Data. Journal of Geophysical Research, 95(D4): 3549-3564.

Goward, S.N., C.J. Tucker, and D.G. Dye. 1985. North American Vegetation Patterns Observed with the NOAA-7 Advanced Very High Resolution Radiometer. Vegetatio, 64 : 3-14.

Goward, S.N., D.G. Dye, A. Kerber, and V. Kalb. 1987. Comparison of North and South American Biomes from AVHRR observations. Geocarto International, 1 : 27-39.

Henricksen, B.L. and J.W. Durkin. 1986. Growing Period and Drought Early Warning in Africa Using Satellite Data. Int.J. Remote Sensing, 7(11): 1583-1608.

Hillel, D. 1971. Soil and Water, Physical Principles and Processes. Academic Press, New York.

Hunt, E.R., Jr., F.C. Martin, and S.W. Running. 1991. Simulating the Effects of Climatic Variations on Stem Carbon Accumulation of a Ponderosa Pine Stand : Comparison with annual growth increment data. Tree Physiology 9: 161-171.

Justice, C.O., J.R.G. Townshend, B.N. Holben, and C.J., Tucker. 1985. Analysis of the Phenology of Global Vegetation Using Meteorological Satellite Data. Int. J. Remote Sensing, 6: 1271-1318.

Justice, C.O., and P.H.Y. Hiernaux. 1986. Monitoring the Grasslands of the Sahel Using NOAA-AVHRR Data : Niger 1983. Int. J. Remote Sensing, 7(11): 1475-1497.

Justice, C.O., T.F. Eck, D. Tanré, and B.N. Holben. 1991. The Effect of Water Vapor on the Normalized Difference Vegetation Index Derived for the Sahelian Region from NOAA-AVHRR Data. Int. J. Remote Sensing, 12(6): 1165-1187.

Kidwell, K.B. 1984. NOAA Polar Orbiter Data (TIROS-N, NOAA-6, NOAA-7 and NOAA-8) User's Guide. National Environmental Satellite Data and Information Service, Washington, D.C.

Lillesand, T. and R. Kiefer. 1987. Remote Sensing and Image Interpretation. J. Wiley, New York.

Malingreau, J.P., G . Stephens, and L. Fellows. 1985. Remote Sensing of Forest Fires : Kalimantan and North Borneo in 1982 - 1983. AMBIO, 14(6): 314-321.

Malingreau, J.P. 1986. Global Vegetation Dynamics : Satellite Observation Over Asia. Int. J. Remote Sensing, 7(9): 1121-1146.

Mather, J.R. 1977. Workbook in Applied Climatology. Publications in Climatology, XXXII(1).

Mather, J.R. 1979. Use of the Climatic Water Budget in Selected Environmental Water Problems. Publications in Climatology, XXXII(1).

Mather, J.R. and C.M. Rowe, Jr. 1979. The Use of the Climatic Water Budget to Evaluate the Validity of a Precipitation Record. Publications in Climatology, XXXII(1).

Mather, J.R. and P.A. Rodriquez. 1979. The Use of the Water Budget in Evaluating Leaching Through Solid Waste Landfills. Publications in Climatology, XXXII(1).

Matson, M. and B. Holben. 1987. Satellite Detection of Tropical Burning in Brazil. Int. J. Remote Sensing. 8(3): 509-516.

Miller, W.A., S.M. Howard, and D.G. Moore. 1986. Use of AVHRR Data in An Information System for Fire Management in The Western United States. Presented at the Twentieth International Symposium on Remote Sensing of Environment, Nairobi, Kenya, 4-10 December 1986.

Monastersky, R. 1991. 'Tis The Season For an El Niño Warming. Science News, 140(24): 389.

Mooney, H.A., C. Field, and C. Vázquez-Yánez. 1984. Photosynthetic Characteristics of Wet Tropical Forest Plants in *Physiological ecology of plants of the wet tropics*. Proceedings of an International Symposium held in Oxatepec and Los Tuxtlas, Mexico, June 29 to July 6, 1983. DR. W. Junk Publishers, Boston : 113-128.

Oldeman, L.R. and M. Frere. 1982. A Study of the Agroclimatology of the Humid Tropics of Southeast Asia. FAO/Unesco/WMO Interagency Project on Agroclimatology. FAO of the United Nations, Rome.

Prince, S.D. 1991. Satellite Remote Sensing of Primary Production: Comparison of Results for Sahelian Grasslands 1981-1988. Int. J. Remote Sensing, 12(6): 1301-1311.

Running, S.W., R.R. Nemani and R.D. Hungerford. 1987. Extrapolation of Synoptic Meteorological Data in Mountainous Terrain and its Use for Simulating Forest Evapotranspiration and Photosynthesis. Can. J. For. Res. 17:472-483.

Running, S.W., and J.C. Coughlan. 1988. A General Model of Forest Ecosystem Processes for Regional Applications. I. Hydrologic Balance, Canopy Gas Exchange and Primary Production Processes. Ecological Modelling, 42: 125-154.

Running, S.W., and R.R. Nemani. 1988. Relating Seasonal Patterns of the AVHRR Vegetation Index to Simulated Photosynthesis and Transpiration of Forest in Different Climates. Remote Sensing of Environment, 24: 347-367.

Running, S.W. 1990. Estimating Terrestrial Primary Productivity by Combining Remote Sensing and Ecosystem Simulation. In Hobbs, R.J. and H.A. Mooney (editors) Remote Sensing of Biosphere Functioning. Springer-Verlag, New York : 66-87.

Schwab, G.O., Richard K.F., Talcott W.E., and Kenneth K.B. 1981. Soil and Water Conservation Engineering. Third Edition. John Wiley & Sons, New York.

Supraptohardjo, Suwardjo, Hardjono A.S., Rahardjo, and Go-Ban Hong. 1966. The Soil Map of Java and Madura. Soil Research Agency, Indonesian Department of Agriculture, Bogor, Indonesia.

Thornthwaite, C.W. and J.R. Mather. 1955. The Water Balance. Publications in Climatology, VIII(1).

Thornthwaite, C.W. and J.R. Mather. 1957. Instructions and Tables for Computing Potential Evapotranspiration and The Water Balance. Publications in Climatology, X(3).

Thornthwaite, C.W., J.R. Mather, and Douglas, B.C. 1958. Three Water Balance Maps of Eastern North America. Resources for The Future, INC., Washington D.C.

Townshend, J.R.G. and C.O. Justice. 1986. Analysis of the Dynamics of African Vegetation Using the Normalized Difference Vegetation Index. Int. J. Remote Sensing, 7(11): 1435-1445.

Townshend, J.R.G., C.O. Justice, and V. Kalb. 1987. Characterization and Classification of South American Land Cover Types Using Satellite Data. Int. J. Remote Sensing, 8(8): 1189-1207.

Tucker, C.J., J.R.G. Townshend, and T.E. Goff. 1985. African Land Cover Classification Using Satellite Data. Science, 227(4685): 369 - 374.

Tucker, C.J., C.O. Justice, and S.D. Prince. 1986. Monitoring the Grassland of the Sahel 1984-1985. Int. J. Remote Sensing, 7(11): 1571-1581.

Whitmore, T.C. 1985. Tropical Rain Forests of the Far East. *Second Edition*. Oxford Science Publications, New York: 53-55.

APPENDICES

Appendix 1. The Climatic Water Balance for Ujung Kulon

A. 1986

Month	P	PE	P-PE	APW	ST	ΔST	AET	D	S	Ro
January	451	123	328		150	0	123	0	328	164
February	260	127	133		150	0	127	0	133	67
March	96	130	-34	-34	119	-31	127	3	0	0
April	95	141	-46	-80	87	-32	127	14	0	0
May	69	139	-70	-150	54	-33	102	37	0	0
June	75	132	-57	-207	37	-17	92	40	0	0
July	186	123	63		100	63	123	0	63	32
August	87	116	-29	-29	123	-27	114	2	0	0
September	154	123	31		150	27	123	0	31	16
October	79	134	-55	-55	103	-47	126	8	0	0
November	304	130	174		150	47	130	0	174	87
December	211	139	72		150	0	139	0	72	36
Total	2067	1557			1373		1353			402

B. 1987

Month	P	PE	P-PE	APW	ST	ΔST	AET	D	S	Ro
January	389	125	264		150	0	125	0	264	132
February	237	123	114		150	0	123	0	114	57
March	132	134	-2	-2	148	-2	134	0	0	0
April	108	142	-34	-36	117	-31	139	3	0	0
May	248	136	112		150	33	136	0	112	56
June	22	142	-120	-120	66	-84	106	36	0	0
July	19	134	-115	-235	31	-35	45	89	0	0
August	18	131	-113	-348	14	-17	35	96	0	0
September	3	140	-137	-485	6	-8	11	129	0	0
October	4	161	-157	-485	2	-4	8	153	0	0
November	50	161	-111	-753	1	-1	51	110	0	0
December	254	136	118		119	118	136	0	118	59
Total	1484	1662			963		1049			304

Appendix 1. (continued)

C. 1988

Month	P	PE	P-PE	APW	ST	ΔST	AET	D	S	Ro
January	206	139	67		150	0	139	0	67	34
February	327	135	192		150	0	135	0	192	96
March	163	139	24		150	0	139	0	24	12
April	197	143	54		150	0	143	0	54	27
May	242	141	101		150	0	141	0	101	51
June	88	135	-47	-47	109	-41	129	6	0	0
July	18	133	-115	-162	50	-59	77	56	0	0
August	68	130	-62	-224	33	-17	85	45	0	0
September	25	141	-116	-340	15	-18	43	98	0	0
October	110	135	-25	-365	13	-2	112	23	0	0
November	182	137	45		58	137	137	0	45	23
December	254	122	132		150	0	122	0	132	66
Total	1880	1630			1178		1402			309

D. 1989

Month	P	PE	P-PE	APW	ST	ΔST	AET	D	S	Ro
January	198	130	68		150	0	130	0	68	34
February	582	114	468		150	0	114	0	468	234
March	62	132	-70	-70	93	-57	119	13	0	0
April	157	135	22		115	22	135	0	22	11
May	122	137	-15	-15	135	20	137	0	0	0
June	50	129	-79	-94	79	-56	106	13	0	0
July	61	133	-72	-166	49	-30	91	42	0	0
August	154	130	24		73	24	130	0	24	12
September	61	133	-72	-72	92	19	80	53	0	0
October	25	145	-120	-192	41	-51	76	69	0	0
November	93	141	-48	-240	30	-11	104	37	0	0
December	259	132	127		150	120	132	0	127	64
Total	1824	1591			1157		1354			355

Appendix 1 (continued)

E. 1990

Month	P	PE	P-PE	APW	ST	ΔST	AET	D	S	Ro
January	488	119	369		150	0	119	0	369	185
February	151	129	22		150	0	129	0	22	11
March	213	131	82		150	0	131	0	82	41
April	140	147	-7	-7	143	-7	147	0	0	0
May	82	141	-59	-66	96	-46	128	13	0	0
June	136	135	1		97	1	135	0	1	1
July	79	124	-45	-45	111	14	93	31	0	0
August	111	128	-17	-62	98	-13	123	5	0	0
September	8	137	-129	-191	41	-57	65	72	0	0
October	74	145	-71	-262	25	-16	90	55	0	0
November	79	149	-70	-332	16	-9	88	61	0	0
December	304	129	175		150	134	129	0	175	88
Total	1865	1614			1227		1377			326

Abbreviations : P = monthly precipitation (mm), PE = monthly potential evapotranspiration (mm), APW = accumulation potential water loss (mm), ST = available water (mm),ΔST = the change of soil moisture (mm), AET = actual evapotranspiration (mm), D = moisture deficit (mm), and S = moisture surplus (mm), Ro = water runoff (mm).

Appendix 2. Monthly Values of Heat Index Corresponding to Monthly Mean Temperature (°C)
(Source : Thornthwaite and Mather, 1957)

T°C	.0	.1	.2	.3	.4	.5	.6	.7	.8	.9
0			.01	.01	.02	.03	.04	.05	.06	.07
1	.09	.10	.12	.13	.15	.16	.18	.20	.21	.23
2	.25	.27	.29	.31	.33	.35	.37	.39	.42	.44
3	.46	.48	.51	.53	.56	.58	.61	.63	.66	.69
4	.71	.74	.77	.80	.82	.85	.88	.91	.94	.97
5	1.00	1.03	1.06	1.09	1.12	1.16	1.19	1.22	1.25	1.29
6	1.32	1.35	1.39	1.42	1.45	1.49	1.52	1.56	1.59	1.63
7	1.66	1.70	1.74	1.77	1.81	1.85	1.89	1.92	1.96	2.00
8	2.04	2.08	2.12	2.15	2.19	2.23	2.27	2.31	2.35	2.39
9	2.44	2.48	2.52	2.56	2.60	2.64	2.69	2.73	2.77	2.81
10	2.86	2.90	2.94	2.99	3.03	3.08	3.12	3.16	3.21	3.25
11	3.30	3.34	3.39	3.44	3.48	3.53	3.58	3.62	3.67	3.72
12	3.76	3.81	3.86	3.91	3.96	4.00	4.05	4.10	4.15	4.20
13	4.25	4.30	4.35	4.40	4.45	4.50	4.55	4.60	4.65	4.70
14	4.75	4.81	4.86	4.91	4.96	5.01	5.07	5.12	5.17	5.22
15	5.28	5.33	5.38	5.44	5.49	5.55	5.60	5.65	5.71	5.76
16	5.82	5.87	5.93	5.98	6.04	6.10	6.15	6.21	6.26	6.32
17	6.38	6.44	6.49	6.55	6.61	6.66	6.72	6.78	6.84	6.90
18	6.95	7.01	7.07	7.13	7.19	7.25	7.31	7.37	7.43	7.49
19	7.55	7.61	7.67	7.73	7.79	7.85	7.91	7.97	8.03	8.10
20	8.16	8.22	8.28	8.34	8.41	8.47	8.53	8.59	8.66	8.72
21	8.78	8.85	8.91	8.97	9.04	9.10	9.17	9.23	9.29	9.36
22	9.42	9 49	9.55	9.62	9.68	9.75	9.82	9.88	9.95	10.01
23	10.08	10.15	10.21	10.28	10.35	10.41	10.48	10.55	10.62	10.68
24	10.75	10.82	10.89	10.95	11.02	11.09	11.16	11.23	11.30	11.37
25	11.44	11.50	11.57	11.64	11.71	11.78	11.85	11.92	11.99	12.06
26	12.13	12.21	12.28	12.35	12.42	12.49	12.56	12.63	12.70	12.78
27	12.85	12.92	12.99	13.07	13.14	13.21	13.28	13.36	13.43	13.50
28	13.58	13.65	13.72	13.80	13.87	13.94	14.02	14.09	14.17	14.24
29	14.32	14.39	14.47	14.54	14.62	14.69	14.77	14.84	14.92	14.99
30	15.07	15.15	15.22	15.30	15.38	15.45	15.53	15.61	15.68	15.76
31	15.84	15.92	15.99	16.07	16.15	16.23	16.30	16.38	16.46	16.54
32	16.62	16.70	16.78	16.85	16.93	17.01	17.09	17.17	17.25	17.33
33	17.41	17.49	17.57	17.65	17.73	17.81	17.89	17.97	18.05	18.13
34	18.22	18.30	18.38	18.46	18.54	18.62	18.70	18.79	18.87	18.95
35	19.03	19.11	19.20	19.28	19.36	19.45	19.53	19.61	19.69	19.78
36	19.86	19.95	20.03	20.11	20.20	20.28	20.36	20.45	20.53	20.62
37	20.70	20.79	20.87	20.96	21.04	21.13	21.21	21.30	21.38	21.47
38	21.56	21.64	21.73	21.81	21.90	21.99	22.07	22.16	22.25	22.33
39	22.42	22.51	22.59	22.68	22.77	22.86	22.95	23.03	23.12	23.21
40	23.30									

Appendix 3. Soil Moisture Retention Table
(Source : Thornthwaite and Mather, 1957)

SOIL MOISTURE RETAINED AFTER DIFFERENT AMOUNTS OF POTENTIAL EVAPOTRANSPIRATION HAVE OCCURRED. WATER HOLDING CAPACITY OF SOIL IS 150 MM.

PE	0	1	2	3	4	5	6	7	8	9
					WATER RETAINED IN SOIL					
0	150	149	148	147	146	145	144	143	142	141
10	140	139	138	137	136	135	134	133	132	131
20	131	130	129	128	127	127	126	125	124	123
30	122	122	121	120	119	118	117	116	115	114
40	114	113	113	112	111	111	110	109	108	107
50	107	106	106	105	104	103	103	102	101	100
60	100	99	98	97	97	97	96	95	94	93
70	93	92	92	91	90	90	89	89	88	87
80	87	86	86	85	84	84	84	83	83	82
90	82	81	81	80	79	79	78	77	77	76
100	76	76	75	75	74	74	73	72	72	71
110	71	71	70	70	69	69	68	68	67	67
120	66	66	66	65	65	64	64	63	63	62
130	62	62	61	61	60	60	60	59	59	58
140	58	58	57	57	56	56	55	55	54	54
150	54	53	53	53	52	52	52	52	51	51
160	51	51	50	50	50	49	49	48	48	47
170	47	47	47	46	46	46	45	45	45	44
180	44	44	44	43	43	43	42	42	42	41
190	41	41	41	40	40	40	40	39	39	39
200	39	38	38	38	37	37	37	37	36	36
210	36	36	35	35	35	35	35	34	34	34
220	34	34	33	33	33	33	33	32	32	32
230	32	31	31	31	31	31	30	30	30	30
240	30	29	29	29	29	29	28	28	28	28

Appendix 3. (continued)

PE	0	1	2	3	4	5	6	7	8	9
					WATER RETAINED IN SOIL					
250	28	27	27	27	27	27	26	26	26	26
260	26	26	25	25	25	25	25	24	24	24
270	24	24	24	23	23	23	23	23	23	23
280	22	22	22	22	22	22	22	22	21	21
290	21	21	21	20	20	20	20	20	20	20
300	20	19	19	19	19	19	19	19	18	18
310	18	18	18	18	18	18	18	17	17	17
320	17	17	17	17	17	17	17	16	16	16
330	16	16	16	16	16	16	16	15	15	15
340	15	15	15	15	15	15	14	14	14	14
350	14	14	14	14	14	14	14	13	13	13
360	13	13	13	13	13	13	13	12	12	12
370	12	12	12	12	12	12	12	12	11	11
380	11	11	11	11	11	11	11	11	11	11
390	11	11	11	10	10	10	10	10	10	10
400	10	10	10	10	10	10	10	10	9	9
410	9	9	9	9	9	9	9	9	9	9
420	9	9	9	8	8	8	8	8	8	8
430	8	8	8	8	8	8	8	8	8	8
440	8	8	8	7	7	7	7	7	7	7

Appendix 4.

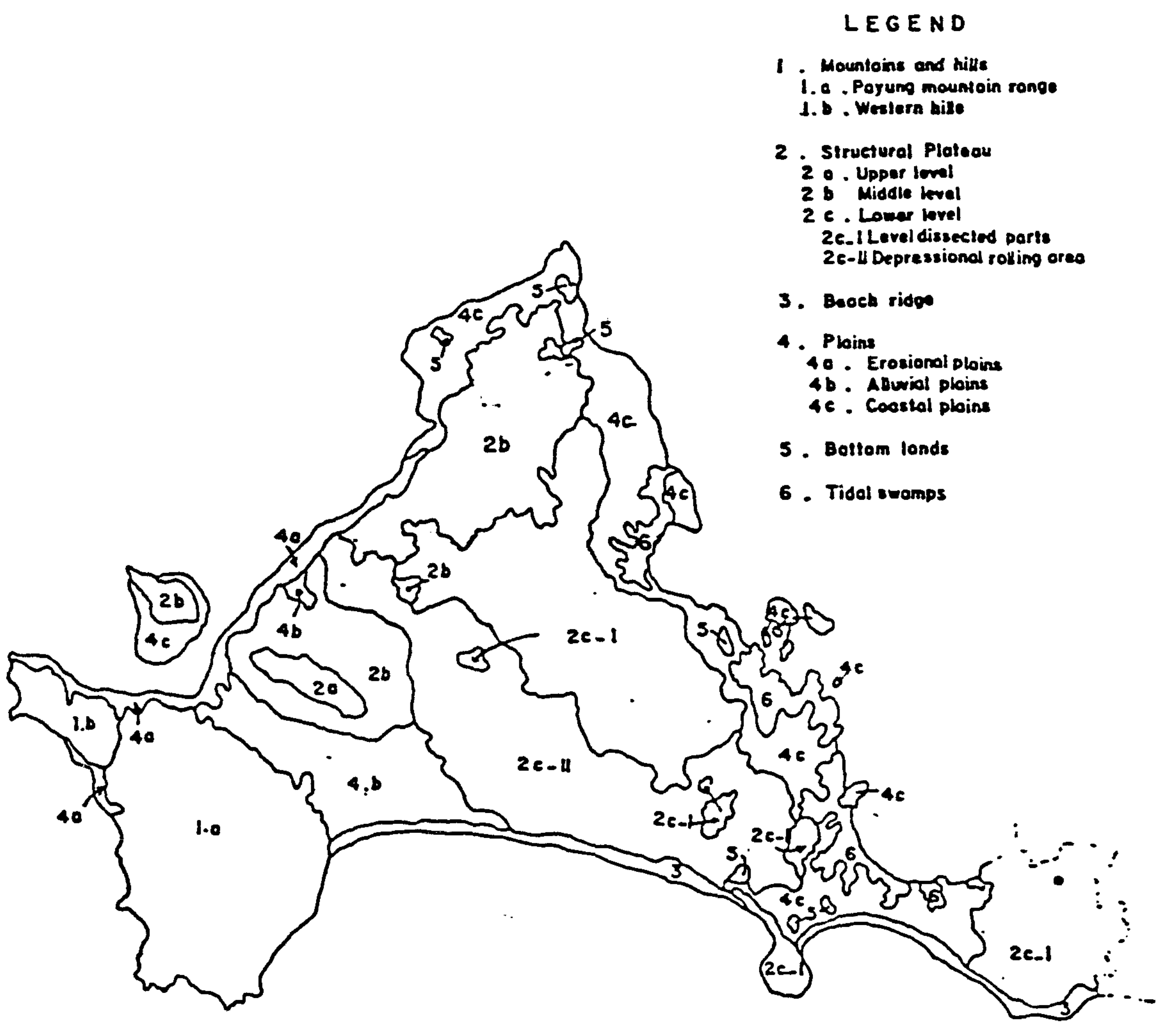

Geomorphological Map of Ujung Kulon
Scale 1 : 150,000
(Source : Anonymous, 1985)

Appendix 5.

Landscape Ecology Map of Ujung Kulon
(Inside Jacket)